

Hyperbranched Supramolecular Polymer of Tris(permethyl- β -cyclodextrin)s with Porphyrins: Characterization and Magnetic Resonance Imaging[†]

Mo Sun, Hengyi Zhang, Xinyue Hu, Bowen Liu, and Yu Liu*

Department of Chemistry, State Key Laboratory of Elemento-Organic Chemistry, Nankai University, Collaborative Innovation Center of Chemical Science and Engineering, Tianjin 300071, China

A hyperbranched supramolecular polymer (HSP) is constructed based on the intermolecular inclusion complexation of bridged tris(permethyl- β -cyclodextrin) with Mn^{III}-porphyrin bearing poly(ethylene glycol) (PEG) side chains (Mn^{III}-TPP), and characterized by UV/vis absorption spectroscopy, isothermal titration calorimetry (ITC), NMR, dynamic light scattering (DLS), atomic force microscopy (AFM) and transmission electron microscopy (TEM), respectively. The presence of permethyl- β -cyclodextrin can stabilize the low-valent Mn^{II}-TPP. *In vitro* cell experiment indicates that this HSP has no remarkable cellular toxicity against NIH 3T3 cells. *In vitro* MR imaging experiment indicates a slightly increased T_1 relaxivity for this HSP compared to that for the linear supramolecular polymer.

Keywords hyperbranched supramolecular polymer, host-guest system, cyclodextrin, Mn-porphyrin, MRI

Introduction

Supramolecular polymers, which combine the advantages of supramolecular chemistry and polymer science, have attracted great attentions in the last few years.^[1] Compared to the conventional covalent polymers, the dynamic nature of non-covalent interactions gives supramolecular polymers a variety of novel features, such as easy processability,^[2] biocompatibility,^[3] stimuli-responsiveness,^[4] and self-healing.^[5] Hyperbranched polymers exhibit the amazing properties of dendrimers through a simply synthetic protocol.^[6] Moreover, some hyperbranched polymers have been used for biomedical applications due to their high biocompatibility.^[7] Hyperbranched supramolecular polymers (HSP), which are constructed by non-covalent interactions while have a same structure as hyperbranched polymers, can unite all the merits from both supramolecular polymers and hyperbranched polymers. However, to date, the reports on the construction of this kind of polymers are still rare.^[8]

Cyclodextrins (CDs), non-toxic supramolecular hosts, are a class of cyclic oligosaccharides with six-eight *D*-glucose units linked by α -1,4-glucose bonds and gain widespread traction in supramolecular polymer chemistry due to their ability to form non-covalent inclusion complexes with hydrophobic guest molecules by host-guest interactions.^[9] Based on our previous works

about the fabrication of supramolecular polymer by CD and porphyrins,^[10] we designed and constructed a new HSP from a CD trimer and Mn-tetrakis(phenyl)porphyrin (Mn-TPP) (Scheme 1), in which the symmetrical bridged tris(permethyl- β -CD)s (**1**) was acted as the core of this HSP (Scheme 2), while Mn-TPP was chosen as the linker for the HSP because of its strong interaction with permethyl- β -CD.^[11] Considering the magnetic resonance imaging (MRI) ability of Mn-TPP^[12] and the advantages when polymers are introduced to MRI contrast agents, such as increasing the relaxivity and solubility,^[13] providing longer blood circulation times,^[14] and displaying a high density of functional ligands (drugs, targeting agents, and imaging agents, *etc.*),^[15] the stabilization of low-valent Mn^{II}-TPP by permethyl- β -CD and the cytotoxicity of HSP were also evaluated. The relaxivity of this HSP was then investigated through *in vitro* MR imaging experiments.

Experimental

General methods and materials

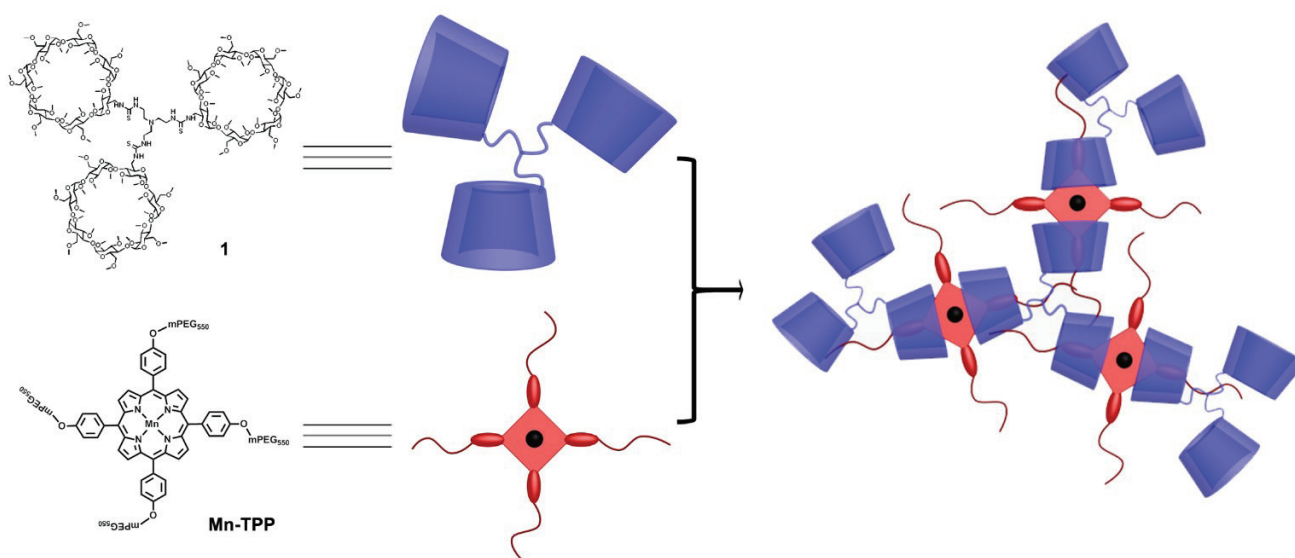
β -Cyclodextrin was purchased and recrystallized from water twice and then dried under vacuum at 85 °C for 24 h before use. Sodium ascorbate was purchased from Aladdin Industrial Company. 2,2',2''-Triaminotriethylamine was purchased from J&K Scientific Com-

* E-mail: yuliu@nankai.edu.cn; Tel.: 0086-022-23503625; Fax: 0086-022-23503625

Received February 18, 2014; accepted March 11, 2014; published online April 22, 2014.

Supporting information for this article is available on the WWW under <http://dx.doi.org/10.1002/cjoc.201400090> or from the author.

[†] Dedicated to Professor Chengye Yuan and Professor Li-Xin Dai on the occasion of their 90th birthdays

Scheme 1 Schematic representation of HSP 1•Mn^{III}-TPP

pany. 6-Deoxy-6-isothiocyanato-permethyl- β -CD and Mn^{III}-TPP were prepared according to the literature procedure. Other chemicals and solvents were commercially available. Column chromatography was performed on silica gel (200–300 mesh).

Instruments

¹H NMR spectra were performed on a Bruker AV400 spectrometer. Mass spectra were performed on an AutoflexIII LRF200-CID (Bruker Daltonics). Elemental analyses were measured by conventional element analyzer. 2D ROESY spectra were performed on a Varian 300 MHz spectrometer. UV/vis spectra were recorded in a quartz cell (light path 10 mm) on a Shimadzu UV-3600 spectrophotometer equipped with a PTC-348WI temperature controller.

ITC measurements

A thermostated and fully computer-operated isothermal calorimetry (VP-ITC) instrument, purchased from Microcal Inc., Northampton, MA, was used for all microcalorimetric experiments. The VP-ITC instrument was calibrated chemically by measurement of the complexation reaction of β -cyclodextrin with cyclohexanol, and the obtained thermodynamic data were in good agreement (error < 2%) with the literature data. All microcalorimetric titrations between **1** and Mn-TPP were performed in aqueous solution at atmospheric pressure and 298.15 K. Each solution was degassed and thermostated by a ThermoVac accessory before the titration experiment. Twenty-six successive injections were made for each titration experiment. A constant volume (10 μ L/injection) of host solution in a 0.250-mL syringe was injected into the reaction cell (1.4227 mL) charged with guest molecule solution in the same aqueous solution. A control experiment was carried out in each run to determine the dilution heat by injecting a host aque-

ous solution into a pure aqueous solution containing no guest molecules. The dilution heat determined in these control experiments was subtracted from the apparent reaction heat measured in the titration experiments to give the net reaction heat.

The net reaction heat in each run was analyzed by using “one set of binding sites” model (ORIGIN software, Microcal Inc.) to simultaneously compute the binding stoichiometry (N), complex stability constant (K_S), standard molar reaction enthalpy (ΔH°) and standard deviation from the titration curve.

AFM measurements

The sample solution was dropped onto newly clipped mica and then dried in air. The samples were performed by using a Multimode Nanoscope-IIIa Scanning Probe Microscope (Digital Instrument Co., Ltd. U.S.A.) in tapping mode in air at room temperature.

TEM measurements

The sample for TEM measurements was prepared by dropping the solution onto a copper grid. The grid was then air-dried. The samples were examined by a high-resolution TEM (Tecnai G² F20 microscope, FEI) equipped with a CCD camera (Orius 832, Gatan) operating at an accelerating voltage of 200 kV.

DLS measurements

The sample solution for DLS measurements was prepared by filtering solution through a 450 nm Millipore filter into a clean scintillation vial. The samples were examined on a laser light scattering spectrometer (BI-200SM) equipped with a digital correlator (Turbo Corr.) at 532 nm at a scattering angle of 90 °C.

Cell culture

Mouse embryonic fibroblast NIH 3T3 cell line was

cultured in the Dulbecco's Modified Eagle's Medium (DMEM) supplemented with 10% fetal bovine serum (FBS) at 37 °C in a humidified atmosphere of 5% of CO₂.

Cytotoxicity studies

The cytotoxicity of **1**·Mn^{III}-TPP was investigated by MTT (3-(4,5-dimethylthiazol-2-yl)-2,5-diphenyltetrazolium bromide, Sigma, St. Louis, MO, USA) viability test on NIH 3T3 cell line. Briefly, cells were plated at a density of 1.0×10^4 cells per well in 96 well. After 24 h incubation, cells were treated by **1**·Mn^{III}-TPP at indicated concentrations for 48 h; then the medium was removed and 200 μ L of fresh medium plus 20 μ L of MTT reagent (2.5 mg dissolved in 50 μ L of DMSO) were added to each well. After incubation for 4 h at 37 °C, the culture medium containing MTT was withdrawn and 200 μ L of DMSO was added, followed by shaking for 10 min until the crystals were dissolved. Viable cells were detected by measuring absorbance at 490 nm using MRX II absorbance reader (DYNEX Technologies, Chantilly, Virginia, USA). The cell growth was expressed as a percentage of absorbance in cells with **1**·Mn^{III}-TPP treatment to that in cells without **1**·Mn^{III}-TPP treatment (100%). The survival rate (IR) was calculated as follows: IR = (A value of **1**·Mn^{III}-TPP well/A value of control well) \times 100%.

MRI relaxivity measurements

The NSP **1**·Mn^{II}-TPP was obtained by adding excess sodium ascorbate into the NSP **1**·Mn^{III}-TPP. The T_1 -weighted images were acquired with a conventional spin echo acquisition (repetition time, TR, 2000 ms) with echo time, TE, of 13 ms in a clinical 3.0 T magnetic resonance scanner (3 T Siemens Magnetom Trio). T_1 relaxivities were measured in a 3.0 T systems (3 T Siemens Magnetom Trio) at room temperature. Relaxivity values of r_1 were calculated through the curve fitting of $1/T_1$ relaxation time (s^{-1}) versus the Mn concentration (mmol/L).

Preparation of **1**

To the solution of 6-deoxy-6-isothiocyanato-per-

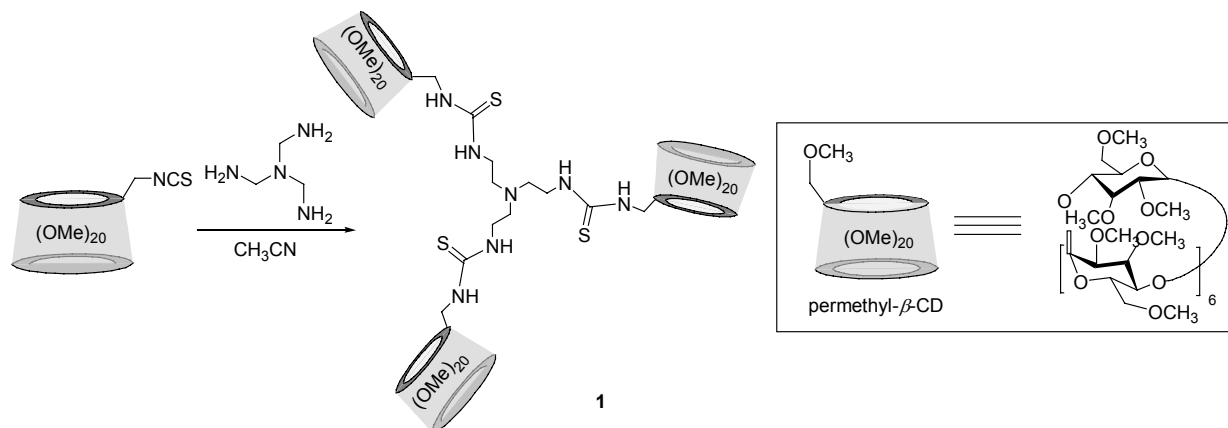
methyl- β -CD (874.0 mg, 0.60 mmol) in acetonitrile (10.0 mL), 2,2',2''-triaminotriethylamine (30.0 μ L, 0.20 mmol) was added under argon atmosphere. The mixture was stirred over night at room temperature. Then the solvent was removed under reduced pressure. The residue was purified by silica gel column by using chloroform-methanol ($V:V=10:1$) to obtain compound **1** as a white solid (65%). ¹H NMR (400 MHz, CDCl₃) δ : 7.27 (s, 3H), 6.28 (s, 3H), 5.24–5.07 (m, 15H), 5.04 (s, 3H), 4.97 (s, 3H), 4.12–3.26 (m, 291H), 3.19 (dd, $J=9.6, 3.3$ Hz, 21H), 2.80 (6, 3H); ¹³C NMR (100 MHz, CDCl₃) δ : 182.6, 99.6, 98.8, 82.0, 81.7, 81.1, 80.1, 71.2, 70.9, 70.9, 61.3, 59.0, 58.6, 58.4, 53.0, 43.5. MS (MALDI) m/z : $[M+Na]^+$ calcd for C₁₉₅H₃₄₅O₁₀₂N₇S₃·Na⁺ 4536.108; found 4536.116. Anal. calcd for C₁₉₅H₃₄₅O₁₀₂N₇S₃: C 51.86, H 7.70, N 2.17; found C 51.78, H 7.73, N 2.19.

Results and Discussion

Bridged tris(permethyl- β -CD)s **1** was obtained by 6-deoxy-6-isothiocyanato-permethyl- β -CD reacted with 2,2',2''-triaminotriethylamine with satisfactory yields (Scheme 2). The HSP was constructed by the complexation of Mn-TPP with **1** in aqueous solution.

UV/vis absorption spectroscopy was employed to investigate the binding behaviours of the two building blocks **1** and Mn-TPP. Upon addition of **1**, the Soret band absorption of Mn^{III}-TPP at 466 nm gradually shifts to shorter wavelength with the increase of intensity (Figure 1), suggesting the formation of the complex between Mn^{III}-TPP and **1**.^[16] Their host-guest binding stoichiometry was investigated using the Job's plot method, where the maximum value of ΔA appeared at a TPP molar fraction of 0.6, representing a 2 : 3 (**1** : Mn^{III}-TPP) stoichiometry (Figure S4). Previous investigations by Kano's and our group have demonstrated that permethyl- β -CD includes water-soluble porphyrins to afford *trans*-type 2 : 1 host-guest complexes. The porphyrin entity acts as a bifunctional linker because of steric constraints between the threaded cyclodextrin rings. Moreover, isothermal titration calorimetry (ITC) measurements supplied the quantitative information for the

Scheme 2 Synthetic route employed for the preparation of **1**



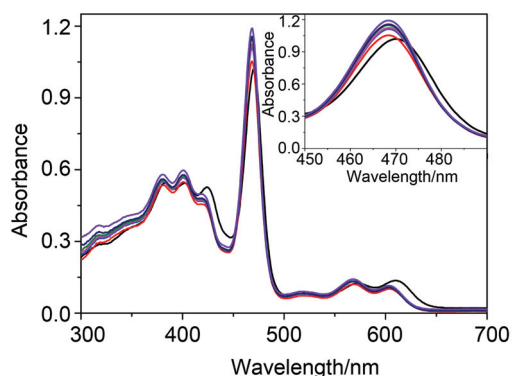


Figure 1 UV/vis spectral changes of $\text{Mn}^{\text{III}}\text{-TPP}$ (1.0×10^{-5} mol/L) in 0.1 mol/L phosphate buffer at pH 7.4 upon addition of **1** at 25 °C. Inset: the magnified area of 450–490 nm.

host-guest complexation (Figures S5 and S6). Fitted using the “one set of binding sites” model,^[8b] the binding stability constant (K_S) value of **1** with $\text{Mn}^{\text{III}}\text{-TPP}$ was $4.642 \times 10^5 \text{ L}\cdot\text{mol}^{-1}$. The experimental “ N ” value of 0.63 (binding molar ratio) closed to the expected value of 0.67 (2 : 3), which was in accordance with the result obtained by the Job’s plot method. To confirm the interaction between **1** and $\text{Mn}^{\text{III}}\text{-TPP}$, NOESY spectral experiment of TPP in the presence of **1** in D_2O was examined. As shown in Figure S7, multiple cross-peaks regarding the protons of $\delta=7.0\text{--}9.0$ assigned to the pyrrole protons with the protons of the secondary OCH_3 of PMCD were observed, indicating that there existed host-guest interactions.

Dynamic laser scattering (DLS), atomic force microscopy (AFM) and transmission electron microscopy (TEM) were subsequently employed to identify the self-assembled size and morphology of the supramolecular polymer. According to the DLS in the Figure S8, the complexation of **1** and $\text{Mn}^{\text{III}}\text{-TPP}$ at a concentration of 0.01 mmol/L formed a spectacular aggregate with an average diameter of 178.4 nm. Neither **1** or $\text{Mn}^{\text{III}}\text{-TPP}$ showed appreciable scattering intensity at the same concentration (Figures S9 and S10), suggesting that no large-size aggregates were formed. When mixing **1** and $\text{Mn}^{\text{III}}\text{-TPP}$ at stoichiometric ratio, a netlike morphology was found in the AFM image (Figure 2).

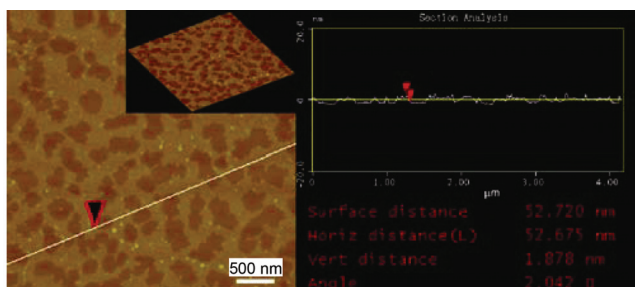


Figure 2 AFM image of the HSP $\mathbf{1}\cdot\text{Mn}^{\text{III}}\text{-TPP}$.

The height of the aggregate was about 1.8 nm, consistent with the size of both **1** and $\text{Mn}^{\text{III}}\text{-TPP}$. Furthermore, the TEM images of the aggregate also showed a fine netlike structure in Figure 3. Both TEM and AFM

images confirmed that the aggregate $\mathbf{1}\cdot\text{Mn}^{\text{III}}\text{-TPP}$ was a supramolecular polymer with a netlike structure. The schematic representation of HSP $\mathbf{1}\cdot\text{Mn}^{\text{III}}\text{-TPP}$ is illustrated in Scheme 1.

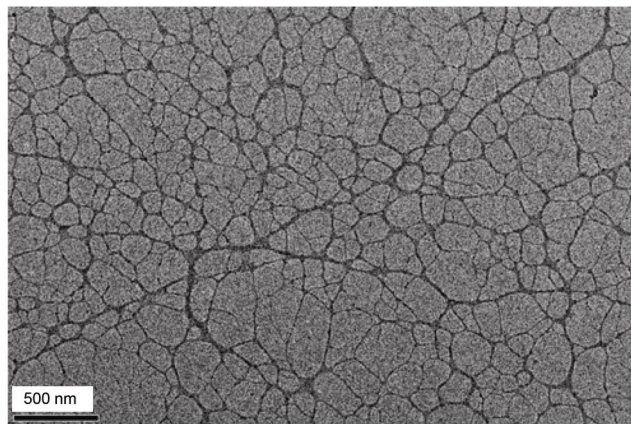


Figure 3 TEM image of the HSP $\mathbf{1}\cdot\text{Mn}^{\text{III}}\text{-TPP}$.

In order to investigate the stability of $\text{Mn}^{\text{II}}\text{-TPP}$, the UV/vis spectral experiments of $\mathbf{1}\cdot\text{Mn}^{\text{III}}\text{-TPP}$ in the presence and absence of excess sodium ascorbate were performed. The absorbances at 466 nm and 434 nm are assigned to Soret band of $\text{Mn}^{\text{III}}\text{-TPP}$ and Soret band of $\text{Mn}^{\text{II}}\text{-TPP}$, respectively.^[17] As shown in Figure S11a, upon addition of sodium ascorbate, a new absorption band of $\mathbf{1}\cdot\text{Mn}^{\text{III}}\text{-TPP}$ remarkably appeared at 434 nm accompanying the absorbance decrease at 466 nm. This observation indicated clearly that sodium ascorbate can reduce Mn^{III} in $\mathbf{1}\cdot\text{Mn}^{\text{III}}\text{-TPP}$ to Mn^{II} effectively. DLS experiment of $\mathbf{1}\cdot\text{Mn}^{\text{II}}\text{-TPP}$ gave the same average diameter of 184.3 nm as the diameter of $\mathbf{1}\cdot\text{Mn}^{\text{III}}\text{-TPP}$ (Figure S8), suggesting that the size of HSP was not influenced significantly by valence states of Mn. Then the stabilization of the HSP $\mathbf{1}\cdot\text{Mn}^{\text{II}}\text{-TPP}$ exposed in air was investigated. In the kinetics experiment, when $\mathbf{1}\cdot\text{Mn}^{\text{II}}\text{-TPP}$ was exposed in air, the autoxidation of $\text{Mn}^{\text{II}}\text{-TPP}$ to $\text{Mn}^{\text{III}}\text{-TPP}$ occurred gradually (Figure S11b). The half-life period was about 30 min in the open air according to the absorbance at 434 nm.

To find useful biological applications, a supramolecular polymer should neither inhibit nor promote the growth of living cells. On the basis of the reduction of 3-(4,5-dimethylthiazol-2-yl)-2,5-diphenyltetrazolium bromide (MTT), cell experiment of HSP was performed on mouse embryonic fibroblast NIH 3T3 cell to evaluate the toxicity. The viability of untreated cells was assumed to be 100%. As shown in Figure 4, cell viability was greater than 80%, whatever the dose (from 1.0×10^{-5} to 1.0×10^{-4} mol/L) used, even after a 48 h exposure. These data show that this HSP can be considered to have low cytotoxicity.

To evaluate the *in vitro* efficiency of this HSP, the longitudinal relaxivities r_1 was obtained with the aid of a 3 T MRI systems utilizing a standard, inversion-recovery sequence at room temperature. Typical

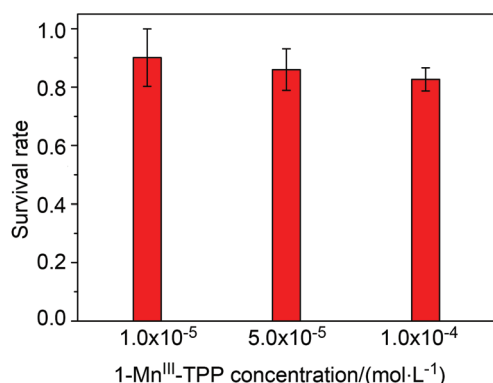


Figure 4 *In vitro* cell viability of NIH 3T3 cells incubated with 1·Mn^{III}-TPP at different concentrations for 48 h.

T_1 -weighted spin-echo MR images recorded for 1·Mn^{II}-TPP at varying Mn^{II} concentrations in water are shown in Figure 5a. Upon gradually increasing the concentration of HSP, a clear positive contrast enhancement of MR signals was observed as revealed by the reinforcement of spot brightness. Quantitative analysis was further conducted to investigate the enhancement of the MR imaging performance (Figure 5b). The HSP 1·Mn^{II}-TPP was found to have longitudinal relaxivity (r_1) of 17.98 mmol⁻¹·L·s⁻¹. Compared to the r_1 value of our previous linear supramolecular polymer,^[18] it was likely that an about 7% increase in the r_1 value of 1·Mn^{II}-TPP was observed. Because this HSP is more rigid than the linear supramolecular polymer, it may have rotational correlation times that are long enough for the water exchange to influence the overall relaxivity.

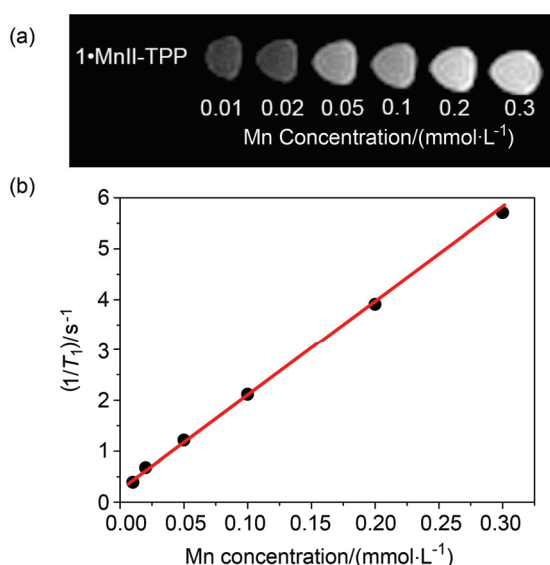


Figure 5 (a) T_1 -Weighted images of 1·Mn^{II}-TPP. (b) Relaxivity plots for 1·Mn^{II}-TPP.

Conclusions

In summary, an HSP was successfully fabricated through the intermolecular inclusion complexation of

Mn^{III}-TPP with bridged tris(permethyl- β -CD) **1**, and it showed a great potential in bioimaging. The binding model of Mn^{III}-TPP with **1** was confirmed by UV/vis spectra, ITC and NMR. The netlike structure of the supramolecular polymer was investigated by DLS, AFM, and TEM analyses. The cavity of permethyl- β -CD played a crucial role in stabilization of low-valent Mn^{II}-TPP according to the UV/vis spectral experiments. The cell experiments showed that this HSP was practically nontoxic. *In vitro* MR imaging characterization exhibited a slightly increased T_1 relaxivity for this HSP compared to that for the linear supramolecular polymer Mn^{III}-TPP with bridged bis(permethyl- β -CD). The research makes progress in constructing different types of the supramolecular polymer, especially constructing a new kind of HSP, and also expanding future application of HSP as a potential MRI contrast agents.

Acknowledgement

We thank the 973 Program (No. 2011CB932500), and the NNSFC (Nos. 20932004, 21372128 and 91227107) for financial support.

References

- (a) Huang, F.; Scherman, O. A. *Chem. Soc. Rev.* **2012**, *41*, 5879; (b) de Greef, T. F. A.; Meijer, E. W. *Nature* **2008**, *453*, 171; (c) Brunsveld, L.; Folmer, B. J. B.; Meijer, E. W.; Sijbesma, R. P. *Chem. Rev.* **2001**, *101*, 4071; (d) Guo, D.-S.; Liu, Y. *Chem. Soc. Rev.* **2012**, *41*, 5907; (e) Harada, A.; Takashima, Y.; Yamaguchi, H. *Chem. Soc. Rev.* **2009**, *38*, 875.
- (a) Folmer, B. J. B.; Sijbesma, R. P.; Versteegen, R. M.; van der Rijt, J. A. J.; Meijer, E. W. *Adv. Mater.* **2000**, *12*, 874; (b) Niu, Z.; Huang, F.; Gibson, H. W. *J. Am. Chem. Soc.* **2011**, *133*, 2836; (c) Park, T.; Zimmerman, S. C. *J. Am. Chem. Soc.* **2006**, *128*, 11582.
- (a) Oohora, K.; Burazerovic, S.; Onoda, A.; Wilson, Y. M.; Ward, T. R.; Hayashi, T. *Angew. Chem., Int. Ed.* **2012**, *51*, 3818; (b) Jin, H.; Huang, W.; Zhu, X.; Zhou, Y.; Yan, D. *Chem. Soc. Rev.* **2012**, *41*, 5986; (c) Bastings, M. M. C.; de Greef, T. F. A.; van Dongen, J. L. J.; Merckx, M.; Meijer, E. W. *Chem. Sci.* **2010**, *1*, 79.
- (a) Yan, X.; Wang, F.; Zheng, B.; Huang, F. *Chem. Soc. Rev.* **2012**, *41*, 6042; (b) Park, J. S.; Yoon, K. Y.; Kim, D. S.; Lynch, V. M.; Bielawski, C. W.; Johnston, K. P.; Sessler, J. L. *Proc. Natl. Acad. Sci. U. S. A.* **2011**, *108*, 20913; (c) Xiao, T.; Feng, X.; Ye, S.; Guan, Y.; Li, S.-L.; Wang, Q.; Ji, Y.; Zhu, D.; Hu, X.; Lin, C.; Pan, Y.; Wang, L. *Macromolecules* **2012**, *45*, 9585; (d) Ge, Z.; Hu, J.; Huang, F.; Liu, S. *Angew. Chem., Int. Ed.* **2009**, *48*, 1798.
- (a) Hentschel, J.; Kushner, A. M.; Ziller, J.; Guan, Z. *Angew. Chem., Int. Ed.* **2012**, *51*, 10561; (b) Fox, J.; Wie, J. J.; Greenland, B. W.; Burattini, S.; Hayes, W.; Colquhoun, H. M.; Mackay, M. E.; Rowan, S. J. *J. Am. Chem. Soc.* **2012**, *134*, 5362; (c) Burnworth, M.; Tang, L.; Kumpfer, J. R.; Duncan, A. J.; Beyer, F. L.; Fiore, G. L.; Rowan, S. J.; Weder, C. *Nature* **2011**, *472*, 334.
- Moers, C.; Nuhn, L.; Wissel, M.; Stangenberg, R.; Mondeshki, M.; Berger-Nicoletti, E.; Thomas, A.; Schaeffel, D.; Koynov, K.; Klappper, M.; Zentel, R.; Frey, H. *Macromolecules* **2013**, *46*, 9544.
- (a) Calderon, M.; Quadir, M. A.; Sharma, S. K.; Haag, R. *Adv. Mater.* **2010**, *22*, 190; (b) Wilms, D.; Stiriba, S.-E.; Frey, H. *Acc. Chem. Res.* **2010**, *43*, 129.
- (a) Alvarez-Parrilla, E.; Cabrer, P. R.; Al-Soufi, W.; Mejjide, F.; Núñez, E. R.; Tato, J. V. *Angew. Chem., Int. Ed.* **2000**, *39*, 2856; (b)

- Tellini, V. H. S.; Jover, A.; García, J. C.; Galantini, L.; Meijide, F.; Tato, J. V. *J. Am. Chem. Soc.* **2006**, *128*, 5728; (c) Liu, Y.; Huang, Z.; Liu, K.; Kelgtermans, H.; Dehaen, W.; Wang, Z.; Zhang, X. *Polym. Chem.* **2014**, *4*, 53; (d) Li, C.; Han, K.; Li, J.; Zhang, Y.; Chen, W.; Yu, Y.; Jia, X. *Chem. Eur. J.* **2013**, *19*, 11892; (e) Fang, R.; Liu, Y.; Wang, Z.; Zhang, X. *Polym. Chem.* **2014**, *4*, 900.
- [9] (a) Chen, G.; Jiang, M. *Chem. Soc. Rev.* **2011**, *40*, 2254; (b) Schmidt, B. V. K. J.; Hetzer, M.; Ritter, H.; Barner-Kowollik, C. *Macromolecules* **2013**, *46*, 1054; (c) Liu, Y.; Chen, Y. *Acc. Chem. Res.* **2006**, *39*, 681; (d) Harada, A.; Kobayashi, R.; Takashima, Y.; Hashidzume, A.; Yamaguchi, H. *Nat. Chem.* **2011**, *3*, 34; (e) Tao, W.; Liu, Y.; Jiang, B.; Yu, S.; Huang, W.; Zhou, Y.; Yan, D. *J. Am. Chem. Soc.* **2012**, *134*, 762.
- [10] (a) Liu, Y.; Ke, C.-F.; Zhang, H.-Y.; Cui, J.; Ding, F. *J. Am. Chem. Soc.* **2008**, *130*, 600; (b) Zhang, Y.-M.; Chen, Y.; Yang, Y.; Liu, P.; Liu, Y. *Chem. Eur. J.* **2009**, *15*, 11333; (c) Gu, Z.-Y.; Guo, D.-S.; Sun, M.; Liu, Y. *J. Org. Chem.* **2010**, *75*, 3600; (d) Zhang, Y.-M.; Chen, Y.; Zhuang, R.-J.; Liu, Y. *Photochem. Photobiol. Sci.* **2011**, *10*, 1393; (e) Wang, K.-R.; Guo, D.-S.; Jiang, B.-P.; Liu, Y. *Chem. Commun.* **2012**, *48*, 3644; (f) Li, Z.-Q.; Zhang, Y.-M.; Guo, D.-S.; Chen, H.-Z.; Liu, Y. *Chem. Eur. J.* **2013**, *19*, 96; (g) Li, Z.-Q.; Zhang, Y.-M.; Chen, H.-Z.; Zhao, J.; Liu, Y. *J. Org. Chem.* **2013**, *78*, 5100.
- [11] (a) Kano, K.; Tanaka, N.; Minamizono, H.; Kawakita, Y. *Chem. Lett.* **1996**, *25*, 925; (b) Kano, K.; Nishiyabu, R.; Yamazaki, T.; Yamazaki, I. *J. Am. Chem. Soc.* **2003**, *125*, 10625; (c) Kano, K.; Kitagishi, H.; Tamura, S.; Yamada, A. *J. Am. Chem. Soc.* **2004**, *126*, 15202; (d) Kano, K.; Kitagishi, H.; Kodera, M.; Hirota, S. *Angew. Chem., Int. Ed.* **2005**, *44*, 435.
- [12] (a) Lee, T.; Zhang, X.-A.; Dhar, S.; Faas, H.; Lippard, S. J.; Jasanoff, A. *Chem. Biol.* **2010**, *17*, 665; (b) Aime, S.; Botta, M.; Gianolio, E.; Terreno, E. *Angew. Chem., Int. Ed.* **2000**, *39*, 747; (c) Caravan, P.; Ellison, J. J.; McMurry, T. J.; Lauffer, R. B. *Chem. Rev.* **1999**, *99*, 2293.
- [13] (a) Floyd, W. C., III; Klemm, P. M.; Smiles, D. E.; Kohlgruber, A. C.; Pierre, V. C.; Mynar, J. L.; Fréchet, J. M. J.; Raymond, K. N. *J. Am. Chem. Soc.* **2011**, *133*, 2390; (b) Datta, A.; Raymond, K. N. *Acc. Chem. Res.* **2009**, *42*, 938; (c) Mishra, R.; Su, W.; Pohmann, R.; Pfeuffer, J.; Sauer, M. G.; Ugurbil, K.; Engelmann, J. *Bioconjugate Chem.* **2009**, *20*, 1860; (d) Ali, M. M.; Woods, M.; Caravan, P.; Opina, A. C. L.; Spiller, M.; Fettingner, J. C.; Sherry, A. D. *Chem. Eur. J.* **2008**, *14*, 7250; (e) Nwea, K.; Bernardo, M.; Regino, C. A. S.; Williams, M.; Brechbiel, M. W. *Bioorg. Med. Chem.* **2010**, *18*, 5925; (f) Song, Y.; Xu, X.; MacRenaris, K. W.; Zhang, X.-Q.; Mirkin, C. A.; Meade, T. J. *Angew. Chem., Int. Ed.* **2009**, *48*, 9143.
- [14] (a) Zhang, Z.; Kolodziej, A. K.; Greenfield, M. T.; Caravan, P. *Angew. Chem., Int. Ed.* **2011**, *50*, 2621; (b) Liu, T.; Li, X.; Qian, Y.; Hu, X.; Liu, S. *Biomaterials* **2012**, *33*, 2521; (c) Li, Y.; Qian, Y.; Liu, T.; Zhang, G.; Liu, S. *Biomacromolecules* **2012**, *13*, 3877; (d) Li, X.; Qian, Y.; Liu, T.; Hu, X.; Zhang, G.; You, Y.; Liu, S. *Biomaterials* **2011**, *32*, 6595; (e) Liu, T.; Qian, Y.; Hu, X.; Ge, Z.; You, Y.; Liu, S. *J. Mater. Chem.* **2012**, *22*, 5020.
- [15] (a) Albertazzi, L.; Fernandez-Villamarin, M.; Riguera, R.; Fernandez-Megia, E. *Bioconjugate Chem.* **2012**, *23*, 1059; (b) Rolland, O.; Turrin, C.-O.; Caminade, A.-M.; Majoral, J.-P. *New J. Chem.* **2009**, *33*, 1809; (c) Tekade, R. K.; Kumar, P. V.; Jain, N. K. *Chem. Rev.* **2009**, *109*, 49; (d) Sakadžić, S.; Roussakis, E.; Yaseen, M. A.; Mandeville, E. T.; Srinivasan, V. J.; Arai, K.; Ruvinskaya, S.; Devor, A.; Lo, E. H.; Vinogradov, S. A.; Boas, D. A. *Nat. Methods* **2010**, *7*, 755.
- [16] Kano, K.; Kitagishi, H.; Sone, Y.; Nakazawa, N.; Kodera, M. *Eur. J. Inorg. Chem.* **2006**, 4043.
- [17] Goldberg, D. P.; Montalban, A. G.; White, A. J. P.; Williams, D. J.; Barrett, A. G. M.; Hoffman, B. M. *Inorg. Chem.* **1998**, *37*, 2873.
- [18] Sun, M.; Zhang, H.-Y.; Liu, B.-W.; Liu, Y. *Macromolecules* **2013**, *46*, 4268.

(Lu, Y.)